Virology 386 (2009) 427–437

Contents lists available at ScienceDirect

Virology

journal homepage: www.elsevier.com/locate/yviro

Kinetics of interaction of Cotton Leaf Curl Kokhran Virus-Dabawali (CLCuKV-Dab) coat protein and its mutants with ssDNA

Poornima Priyadarshini C. G., H.S. Savithri *

Department of Biochemistry, Indian Institute of Science, Bangalore 560012, India

ARTICLE INFO

Article history:
Received 27 November 2008
Returned to author for revision
23 December 2008
Accepted 15 January 2009
Available online 23 February 2009

Keywords:
Geminiviridae
Begomoviruses
Cotton Leaf Curl Kokhran Virus (CLCuKV)
Coat protein
Surface plasmon resonance
ssDNA interaction
Zinc finger motif

ABSTRACT

Gemini viral assembly and transport of viral DNA into nucleus for replication, essentially involve DNA-coat protein interactions. The kinetics of interaction of *Cotton Leaf Curl Kokhran Virus-Dabawali* recombinant coat protein (rCP) with DNA was studied by electrophoretic mobility shift assay (EMSA) and surface plasmon resonance (SPR). The rCP interacted with ssDNA with a K_A, of $2.6 \pm 0.29 \times 10^8\ M^{-1}$ in a sequence non-specific manner. The CP has a conserved C2H2 type zinc finger motif composed of residues C68, C72, H81 and H85. Mutation of these residues to alanine resulted in reduced binding to DNA probes. The H85A mutant rCP showed the least binding with approximately 756 fold loss in the association rate and a three order magnitude decrease in the binding affinity as compared to rCP. The CP–DNA interactions via the zinc finger motif could play a crucial role in virus assembly and in nuclear transport.

Introduction

The *Geminiviridae* family of plant viruses infect both monocotyledonous and dicotyledonous plants and cause significant yield loss in many crops worldwide. They are classified into four genera (*Mastrevirus*, *Curtovirus*, *Topocuvirus* and *Begomovirus*) depending on their genomes, insect mode of transmission and host range (Stanley et al., 2005; Van Regenmortel et al., 2000). These viruses contain one or two circular ssDNA molecules of size 2.5–3 kb as their genome. Begomoviruses form the largest genus among the *Geminiviridae* family. They infect dicotyledonous plants and are transmitted by the whitefly, *Bemisia tabaci*. Begomoviruses are either bipartite with two genomic components, designated as DNA-A and DNA-B or monopartite with only DNA-A (Lazarowitz, 1992). Some of the monopartite begomoviruses are also associated with additional circular ssDNA molecules, such as DNA-β or DNA-1 that are nearly half the size of DNA-A and these satellite DNA molecules are reported to be involved in symptom attenuation (Briddon, 2003; Briddon et al., 2003, 2004). DNA-A has the potential to code for six gene products. AV1 and AV2 are encoded by the virion-sense strand whereas AC1, AC2, AC3 and AC4 are coded by virion complimentary-sense strand. AV1 or the coat protein (CP) is the only protein necessary for virus assembly. AV2 is suggested to be important for cell to cell movement of the virus (Padidam et al., 1996). AC1 and AC3 are involved in viral replication. AC2 and AC4 are essential for transcriptional activation of viral genes and in symptom development respectively (Lazarowitz, 1992). Recently, these proteins have been shown to function as suppressors of gene silencing (Bisaro, 2006; Gopal et al., 2007). DNA-B encodes two gene products namely BV1 and BC1 from the sense strand and the complimentary-sense strand respectively that are essentially involved in viral movement (Lazarowitz, 1992; Stanley and Townsend, 1985).

Geminiviruses have a unique architecture in which two incomplete $T=1$ icosahedra are joined together to form geminate particles consisting of 22 pentameric capsomers made of 110 identical CP subunits (Bottcher et al., 2004; Hatta and Francki, 1979; Zhang et al., 2001). One molecule of the DNA genome is encapsidated within each geminate particle. In addition to its pivotal role in the assembly of geminate particles (Bottcher et al., 2004; Hallan and Gafni, 2001; Lazarowitz, 1992; Zhang et al., 2001), the CP is involved in insect transmission, virus movement and host plant infection (Azzam et al., 1994; Hofer et al., 1997; Hohnle et al., 2001; Noris et al., 1998; Wartig et al., 1997). Further, the nuclear localization signal (NLS) sequence present in the N-terminal region of CP is shown to be involved in the transport of viral DNA into the nucleus (Kunik et al., 1998; Palanichelvam et al., 1998). Studies on *Tomato yellow leaf curl virus* (TYLCV) CP have suggested that the CP also mediates the export of ss- and dsDNA (Rojas et al., 2001). Hence, it can be concluded that the geminiviral CP is multifunctional.

The CP of some of the members of the *Geminiviridae* family such as *Abutilon mosaic virus* (AbMV), *Maize streak virus* (MSV), *Tomato leaf*

* Corresponding author. Fax: +91 80 2360 0814.
E-mail address: bchss@biochem.iisc.ernet.in (H.S. Savithri).

0042-6822/$ – see front matter © 2009 Elsevier Inc. All rights reserved.
doi:10.1016/j.virol.2009.01.016

curl Bangalore virus (ToLCBV-Ban5) and TYLCV have been overexpressed in *E. coli* and characterized (Hehnle et al., 2004; Kirthi and Savithri, 2003; Liu et al., 1997; Palanichelvam et al., 1998; Wege and Jeske, 1998). In all these cases, the protein was present in the insoluble fraction and the refolded protein was used for studies on protein–protein and protein–DNA interactions. It was demonstrated by an analysis of deletion mutants of TYLCV that there was a head to tail homotypic interaction between CP subunits (Hallan and Gafni, 2001). It was also shown that TYLCV CP binds cooperatively to ssDNA in a sequence non-specific manner (Palanichelvam et al., 1998). Deletions of the nuclear targeting sequences present at the N-terminus of the *African cassava mosaic virus* (ACMV) CP prevented twinned particle assembly (Unseld et al., 2004). The CP of MSV was shown to interact with ssDNA and dsDNA in a sequence non-specific manner and the DNA binding domain was localized to the N-terminal half of the protein (Liu et al., 1997).

The monopartite begomoviruses are major plant pathogens infecting a number of crop plants in India. In an earlier study, we have established the genetic variability in the DNA-A sequences of begomoviruses causing Tomato leaf curl disease (Kirthi et al., 2002) and Cotton leaf curl disease (Kirthi et al., 2004). Further, ToLCBV-Ban5 CP was shown to bind to ssDNA in a sequence non-specific manner and a conserved C2H2 type zinc finger motif was shown to be responsible for such an interaction (Kirthi and Savithri, 2003). However, the CP was purified from the insoluble fraction and hence, it precluded detailed quantitative analysis of DNA–protein interaction. Other well characterized proteins with C2H2 zinc finger motifs are transcription factors, such as TFIIIA and kruppel (Klug and Schwabe, 1995). Such motifs have been shown to be involved in protein–DNA/RNA and protein–protein interactions (Mackay and Crossley, 1998; Shastry, 1996).

In most of the studies of CP–DNA interactions of geminiviruses, electrophoretic mobility shift assays (EMSA), slot blot analysis or south Western analysis has been used (Kirthi and Savithri, 2003; Liu et al., 1997; Palanichelvam et al., 1998). These methods do not permit accurate measurements of binding constants. Surface plasmon resonance (SPR) experiments detect real time complex formation. The association (on) and dissociation (off) rates for the molecular interaction can be obtained from the sensorgram recorded (Bondeson et al., 1993; Myszka, 2000; Nice and Catimel, 1999; Oda et al., 1999; Tsoi and Yang, 2002). The method offers a reliable and rapid determination of rate and equilibrium constants and enables measurement of association rates ranging from 10^3 to 10^7 M^{-1} s^{-1} and dissociation rates from 10^{-1} to 10^{-5} s^{-1} (Hensley et al., 2000; Myszka, 2000; O'Shannessy, 1994; Yoshioka et al., 1999). It also permits a quantitative analysis of the binding constants for various mutants (Garland, 1996; Silin and Plant, 1997). SPR studies on protein–DNA interactions have been reported earlier. In the case of ADR1 zinc finger transcription factor, the mechanism of DNA binding has been characterized using this technique with wild type and mutant proteins (Oda et al., 1999; Yamamoto et al., 1997; Yoshioka et al., 1999). Sequence-specific binding of nucleocapsid protein of Human Immunodeficiency Virus Type 1 (HIV-1) to short oligonucleotides has also been extensively studied using SPR (Fisher et al., 1998, 2006).

In the present study, the CP of *Cotton Leaf Curl Kokhran Virus-Dabawali* (CLCuKV-Dab) (Kirthi et al., 2004) was overexpressed in *E. coli* and purified from the soluble fraction by differential centrifugation and sucrose density gradient centrifugation. Using EMSA and SPR, the DNA binding properties of the CLCuKV-Dab recombinant CP (rCP) were examined. The binding affinity of rCP to oligonucleotide as measured by SPR was found to be $2.6 \pm 0.29 \times 10^8$ M^{-1}. Site-directed mutagenesis of the residues C68, C72, H81 and H85 in the conserved zinc finger motif to alanine resulted in reduced binding of the mutant rCPs to DNA probes and the H85A mutant rCP showed the least binding affinity of $1.7 \pm 0.49 \times 10^5$ M^{-1}.

Results

Expression and solubility analysis of rCP

The CLCuKV-Dab AV1 ORF encodes CP of molecular mass ~29 kDa. The CP gene amplified by PCR was cloned into pRSET C and the pR-CP clone was overexpressed in *E. coli* BL21 (DE3) pLys S cells as described in the Materials and methods section. The expression of rCP was checked by SDS-PAGE. Cells transformed with the vector alone served as negative control. The rCP showed a molecular mass of 32 kDa corresponding to 256 amino acids from CP gene, 18 vector derived amino acids including a hexahistidine-tag at the N-terminus and two additional amino acids at the C-terminus (Fig. 1A, lane 4). As expected, no protein band corresponding to the size of CP was observed in the negative control (Fig. 1A, lanes 1 and 2). Although the expression level of rCP was high, the protein was present mostly in the insoluble fraction. Several modifications were made in the growth conditions and in the lysis buffer to improve the solubility. Approximately 15–20% of the overexpressed rCP was found to be soluble when induced at 30 °C and lysed in 50 mM sodium acetate buffer (pH 5.5), containing 10% glycerol and 1% Triton X-100, as evident from the SDS PAGE Fig. 1B (gel stained with Coomassie blue, lane S) and Western blot analysis (Fig. 1C, lane S).

rCP purification

The soluble fraction of rCP was initially purified by differential centrifugation. This was followed by sucrose density gradient (10–40%) centrifugation. Fractions (1.5 ml each) were collected and analyzed by measuring the absorbance at 280 nm. The cells transformed with pRSET C and uninduced cells transformed with pR-CP were processed in parallel as controls. As shown in Fig. 2A, a peak was observed between the fractions 10–14 in the overexpressed soluble rCP sample whereas no such peak was observed in the controls. SDS PAGE (Fig. 2B, gel stained with Coomassie blue) and Western blot analysis of the rCP fractions (Fig. 2C) showed that the rCP was predominantly present in fractions 10–14. These fractions were pooled and subjected to ultracentrifugation. The pellet obtained was resuspended in minimum volume of 50 mM sodium acetate buffer, pH 5.5 and the purity of the protein was checked by SDS-PAGE. A major band with the expected molecular mass of rCP (32 kDa) (Fig.

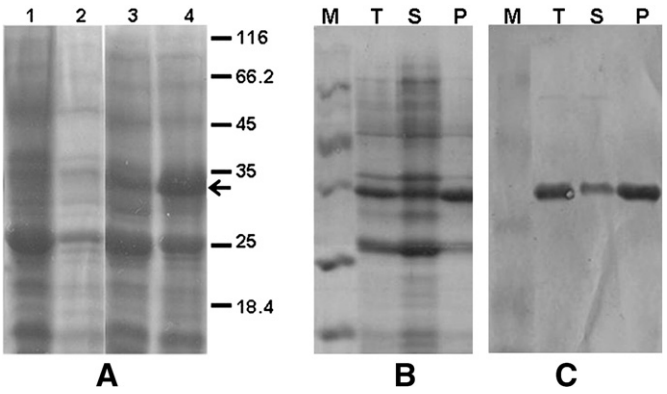

Fig. 1. Expression and solubility analysis of rCP. (A) The CLCuKV-Dab pR-CP and pRSET C vector as control were transformed into *E. coli*. Total lysate from both cells after IPTG induction was analyzed on 12% SDS PAGE and stained with Coomassie Brilliant Blue R250. Lanes 1 and 2 show uninduced and induced total lysate of pRSET C respectively and lanes 3 and 4 correspond to uninduced and induced cell lysates of pR-CP transformed cells respectively. Arrow indicates the position of rCP band in the induced sample in lane 4. (B) SDS PAGE (12%) of total (T), soluble (S) and the pellet (P) fractions of pR-CP expressing cells to test for the solubility of rCP. The gel was stained with Coomassie Brilliant Blue R250. M, protein molecular mass markers and (C) Western blot analysis of the same fractions with ICMV polyclonal antibodies. M. Prestained molecular mass markers T, S, and P correspond to total, soluble and pellet fractions respectively.

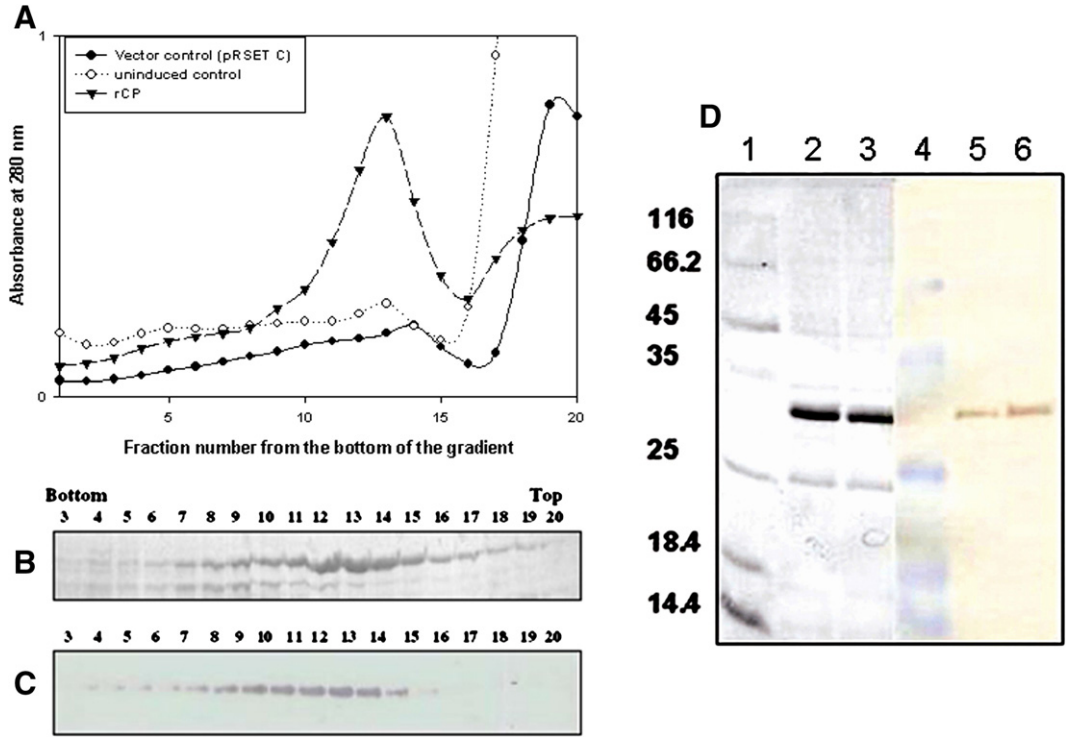

Fig. 2. Sucrose density gradient analysis. (A) Soluble fraction from uninduced and induced cell cultures of pR-CP transformed cells and the induced cells transformed with pRSET C as control were subjected to sucrose density gradient analysis. Fractions (1.5 ml) were collected from the bottom of the tube; the absorbance at 280 nm was measured and plotted against fraction number. (B) The fractions (of the soluble fraction of rCP expressing cell lysate) from 10–40% sucrose density gradient were subjected to 12% SDS-PAGE analysis. The gel was stained with Coomassie Brilliant Blue R250. (C) The presence of rCP was confirmed by Western blot analysis using ICMV polyclonal antibodies. (D) The fractions containing rCP (10–14) were pooled, ultrapelleted and analyzed on 12% SDS-PAGE and stained with Coomassie Brilliant Blue R250 and a duplicate gel was subjected to Western blot analysis using ICMV polyclonal antibodies. Lane 1, protein molecular mass marker; lanes 2 and 3 purified rCP (in duplicate) stained with Coomassie blue R250. Lane 4, prestained protein molecular mass markers; Lanes 5 and 6 represent the Western blot of purified rCP (in duplicate).

2D, lanes 2 and 3) was observed which cross reacted with *Indian cassava mosaic virus* (ICMV) polyclonal antibodies (Fig. 2D, lanes 5 and 6). In addition, a minor band at 25 kDa was also observed. This partially purified rCP was used for studies on DNA binding properties of the protein. The yield of the purified protein was 1–2 mg/l culture.

rCP–DNA interaction

Earlier studies on ToLCBV-Ban5 CP had shown that it bound to ssDNA in a sequence non-specific manner (Kirthi and Savithri, 2003). It was therefore of interest to examine whether the rCP could bind to DNA. rCP (500 ng) was incubated separately with end labeled AV1S probe (corresponding to the 5′ terminal nucleotides of the AV1 ORF encoding the CP gene), dsCP probe obtained by annealing AV1S primer with an antisense primer corresponding to AV1S complementary sequence and a non-viral DNA probe, such as M13 sense primer for 20 min at 4 °C and EMSA was performed by running the samples on 6% native PAGE as described in the Materials and methods section. Interestingly, rCP interacted with AV1S ssDNA (Fig. 3A, lane 3) and it did not bind to dsCP probe or the M13 probe (Fig. 3A, lanes 4 and 5). Further, to confirm that the mobility shift observed was indeed due to the rCP–DNA interaction, the rCP–AV1S complex was incubated with ICMV polyclonal antibodies, which resulted in the super shift of the rCP–AV1S complex on native PAGE due to the formation of ternary complex (Fig. 3B). Such a supershift was not observed when preimmune serum was used (data not shown). With the increase in the concentration of the antibody, there was an increase in the intensity of the ternary complex (Fig. 3B, lanes 4–6). Yet another confirmation was obtained from competition experiments, in which the rCP–AV1S complex formed was incubated with the unlabeled AV1S, dsCP and M13S oligonucleotides separately and EMSA was carried out. M13S and dsCP probes did not chase the label (Fig. 3C, lanes 5 and 6) whereas AV1S was able to chase the label in the complex completely (Fig. 3C, lane 4). Thus, interestingly, rCP bound to AV1S but not to M13S even though both were ssDNA oligonucleotides. Further, the effect of rCP concentration (0–500 ng) on the complex formation was tested. As evident from Fig. 4A (Lanes 4–7), the rCP–DNA interaction was concentration dependent. The fraction of bound DNA was quantified by estimating the intensity of the retarded band and comparing it to the total intensity of the bound and free probes. The fraction of bound DNA was plotted as a function of rCP concentration and the sigmoid nature of the curve suggested that the binding was cooperative (Fig. 4B). Similar results were obtained earlier with TYLCV CP (Palanichelvam et al., 1998).

In order to probe further into the specificity of rCP–DNA interaction, ssDNA oligonucleotides (Table 1) corresponding to 5′ (sense) and 3′ (antisense) terminal region of AV1, AV2, AC1, AC2, AC3 and AC4 ORFs as well as intergenic region (IRstem, IR112nt) of DNA-A were chosen to represent different regions of the genome (Fig. 5A). The fraction of bound DNA when these probes were used individually with rCP (500 ng) is shown as bar diagram (Fig. 5B). Appreciable binding was observed with all the probes tested (Fig. 5B). Interestingly, rCP could bind to both sense and antisense probes of viral origin and when the sequences of the probes (Table 1) were analyzed; a TT-stretch was present in all the oligonucleotides used except in M13S, which also did not bind to rCP. To test if TT stretch had a role to play in binding, oligonucleotides were designed such that in the M13S, a TT was introduced (M13S + TT) and in the AV1S the TT was removed (AV1S − TT), keeping the overall base composition of the oligonucleotides the same. Non-viral oligonucleotide (NG6 − TT 32mer) of length equal to that of AV1S was also tested. As shown in Fig. 5C, the rCP bound to all the probes except M13S. Although the rCP could bind M13S + TT, it also bound to AV1S − TT and to NG6 − TT 32mer oligonucleotides that did not have a TT. These results suggested that

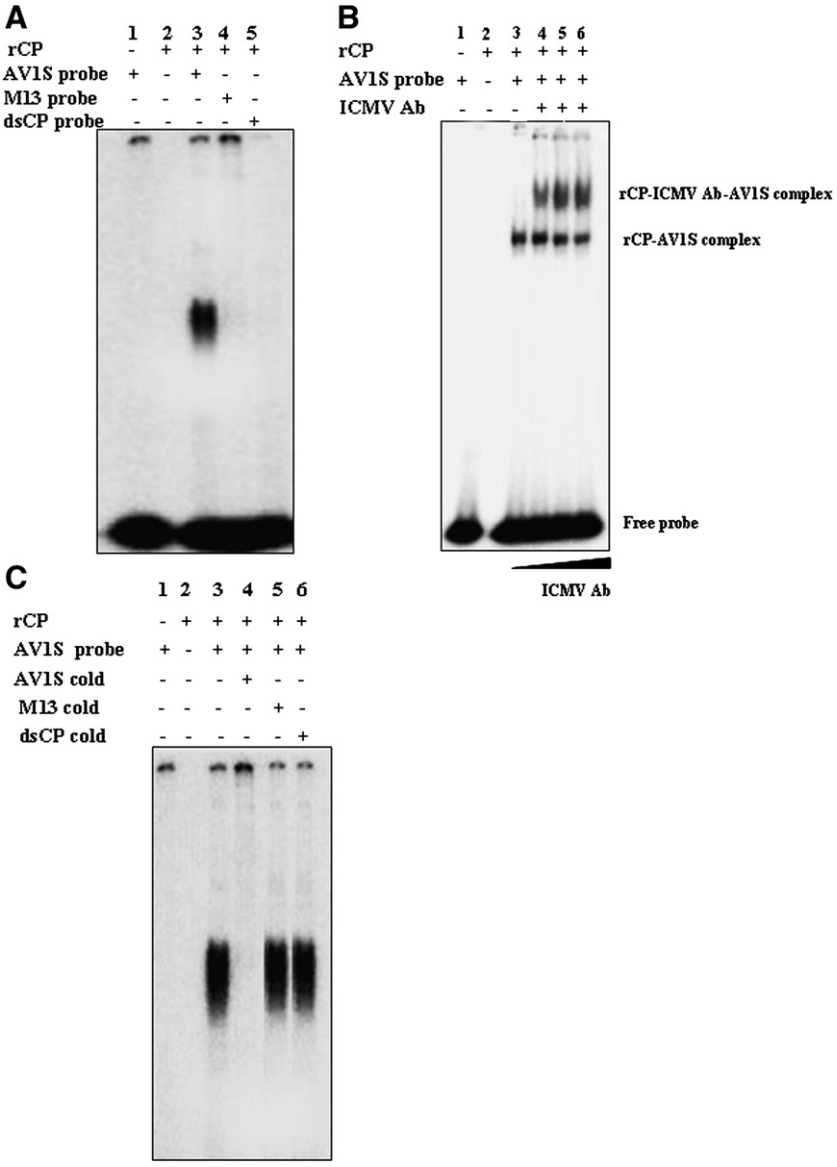

Fig. 3. rCP interaction with ssDNA probes. (A) EMSA was performed by incubating rCP (500 ng) with indicated radiolabeled probes (10,000 cpm) individually and analyzing the samples on 6% Native PAGE followed by phosphorImaging. Lane 1, AV1S probe alone; lane 2, rCP control and lanes 3, 4 and 5 represent AV1S, M13S and dsCP probes with rCP respectively. (B) Super shift assay. rCP–DNA complex was further incubated with (+) or without (−) ICMV polyclonal antibodies to observe the super shift due to the formation of AV1S, rCP and antibody ternary complex . Lane 1, AV1S probe; lane 2, rCP control. Lane 3, AV1S + rCP; lanes 4, 5 and 6, AV1S + rCP + increasing concentrations (1:100, 1:50 and 1:25 dilutions) of ICMV polyclonal antibodies. (C) Competition EMSA: Unlabeled specific (AV1S, lane 4) or non-specific ssDNA (M13S, lane 5) and dsCP probes (lane 6) (1000 molar excess) were incubated with rCP–AV1S (labeled) complex and EMSA was performed. The samples were electrophoresed on native PAGE, and visualized by phosphorImaging.

rCP does not necessarily recognize TT and that the binding to ssDNA is sequence non-specific.

Role of zinc-finger motif in DNA binding

The amino acid sequence of CLCuKV-Dab CP was compared with other begomoviral CP sequences using multiple sequence alignment (Fig. 6A). CLCuKV-Dab CP has conserved cysteine and histidine residues (C68, C72, H81 and H85) that could possibly form a zinc finger motif at its N-terminus (Fig. 6B). These residues were mutated to alanine by PCR based site directed mutagenesis (Weiner et al., 1994) and the mutants were purified as described in the Materials and methods section. The yield of the mutant rCPs was in the range of 1–2 mg/l culture. The rCP mutants were tested for their ability to bind to ssDNA as described earlier for the wild type rCP. As shown in the Fig. 6C, all the rCP mutants showed reduced level of binding to AV1S DNA probe compared to wild type rCP when equated protein (500 ng) and input counts (10,000 cpm) were used in all the samples. H85A mutant showed the least binding (Fig. 6C, lane 7).

SPR studies

The EMSA data presented thus far clearly indicates that the rCP interacts with ssDNA probes. In order to quantitate these interactions, SPR was performed. For this purpose, 5′ biotinylated AV1S oligonucleotide was immobilized on BIAcore SA sensor chips and SPR experiments were conducted at 25 °C with different rCP concentrations (0–250 nM). The sensorgram obtained depicts change in response units (RU) as a function of time (S). The amplitude of the RU signal is directly proportional to the amount of protein bound to the chip. As shown in Fig. 7, the rCP bound rapidly to AV1S oligonucleotide at low concentrations (0.5–10 nM) and the association and dissociation were concentration dependent. However, at higher concentrations (above 15 nM), although an increase in association was observed

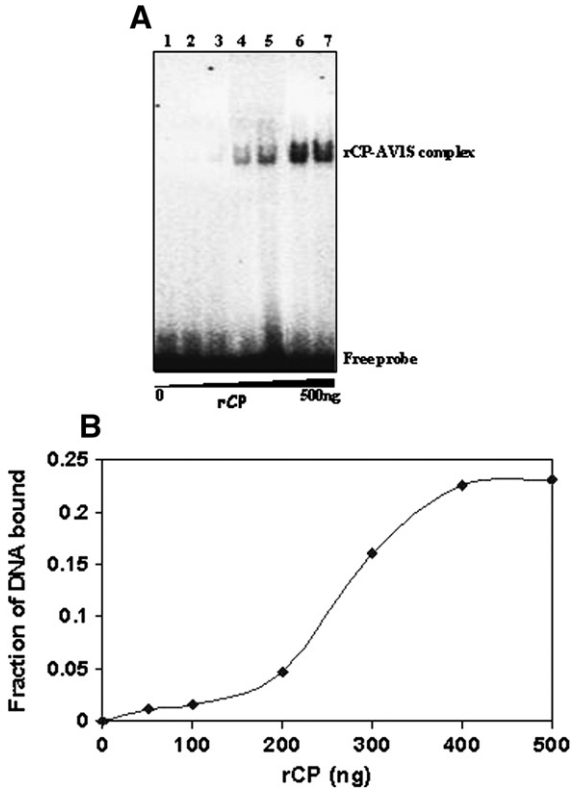

Fig. 4. Nature of rCP–DNA interaction. (A) The labeled probe was incubated with increasing amounts of rCP, and the complex was electrophoresed on native PAGE. A significant increase in the intensity of the retarded band was observed with increase in the rCP concentration. (B) The fraction of bound DNA quantified as described in the Materials and methods section was plotted as a function of rCP concentration.

the dissociation curves were more steep showing that there was additional binding of rCP to AV1S but with lower affinity (Figs. 7A and B). These results indicated that the saturation of the interaction was reached by 15 nM of rCP concentration. The interaction was further authenticated by performing SPR with immunodepleted fraction that would be devoid of rCP. The sensorgram clearly showed that such a fraction failed to bind to AV1S (Supplementary Fig. S1).

In order to determine the binding constants for rCP and the mutants, the biosensor analysis was carried out. As shown in Fig. 8A, Table 2 and summarized in Fig. 8B, there was a difference in the association rates for the wild type and the mutant rCPs, while the dissociation rates appeared to be relatively unaffected. The rCP showed a k_a of $1.3 \pm 0.18 \times 10^6$ M^{-1} s^{-1} and a k_d of $4.9 \pm 1.23 \times 10^{-3}$ s^{-1}, from which the binding affinity K_A and the dissociation constant K_D were calculated to be $2.6 \pm 0.29 \times 10^8$ M^{-1} and $3.8 \pm 0.43 \times 10^{-9}$ M respectively. Compared to rCP, H85A mutant showed 756 fold decrease in k_a value. Additionally, the mutation severely reduced the DNA binding, decreasing the affinity by three orders of magnitude. H81A and C72A mutations led to approximately 9- and 33-fold reduction in binding affinity and 23- and 50-fold decrease in association rates respectively. However, for the C68A mutant, the reduction in affinity and the association rate were by two orders of magnitude.

Discussion

A distinguishing feature of members of *Geminiviridae* family is that their circular ss DNA genome is encapsidated in geminate particles consisting of two incomplete icosahedra formed by 110 identical CP subunits. It has not been possible to study the assembly of geminiviruses mainly because of the difficulty in purification of these viruses from infected plant material in sufficient amounts. In many icosahedral viruses, the expression of CP in heterologous

Table 1
List of oligonucleotides used for EMSA, SPR studies and sense (s) and antisense (a) used for site directed mutagenesis (5′–3′)

EMSA and SPR studies		
IRstem (2740–12)	CGGACATCCGCATAATATTACCGGATGGCCGC	Corresponds to Inter genic (IR) stem loop region
IR112nt (111–143)	AAGTACTTCGTTGCTAAGTATGCGTTTGAAAA	Intergenic region (IR)
AV1S (304–336)	ATGTCGAAGCGACCAGCAGATATAATCATTTC	5′ terminal of CP gene in the sense orientation
AV1A (1042–1074)	TAATTTGTCACGGAATCATAGAAGTAGATCCGT	3′ terminal of CP gene in the antisense orientation
AV2 S (144–176)	ATGTGGGATCCACTGTTAAATGAGTTCCCCGA	5′ terminal of AV2 gene in the sense orientation
AV2A (468–500)	GGAACATCTTGGACTTCTGTACATCCTGTACA	3′ terminal of AV2 gene in the antisense orientation
AC1S (2605–2637)	ATGCATCCGAAACGTTTTGTTATTAACCAAAA	5′ terminal of AC1 gene in the antisense orientation
AC1A (1491–1523)	ACTCTCCGACGTCTGGTCCCCTTCTTGGCTAG	3′ terminal of AC1 gene in the sense orientation
AC2S (1620–1652)	ATGCAATCTTCATCACCCTCGAGAGCCCACTC	5′ terminal of AC2 gene in the antisense orientation
AC2A (1184–1216)	AAGACCCTTAAGAAACGACCAGTCGGAGGCT	3′ terminal of AC2 gene in the sense orientation
AC3S (1475–1507)	ATGGATTCACGCACAGGGGAACCCATCACTGC	5′ terminal of AC3 gene in the antisense orientation
AC3A (1039–1071)	ATAAATATTGAATTTTATTGAAGATGATTGGT	3′ terminal of AC3 gene in the sense orientation
AC4S (2451–2483)	GGGAACCTCATATTCACGTGCTCATCCAGTTC	5′ terminal of AC4 gene antisense orientation
AC4A (2117–2149)	ATGGTTCCTTAATGACTCTAAGAGCCTCCGAC	3′ terminal of AC4 gene in the sense orientation
M13 S	TGTAAAACGACGGCCAGTGCCAAGCTCCCGCG	M13 promoter region primer sequence
M13S + TT	TGAAAACGACGGCCAGTTTGCCAAGCCCCGCG	M13 promoter region primer sequence with 'TT' introduced, keeping the base composition same.
AV1S − TT	ATGTCGAAGCGTACCAGTCAGATATAATCATC	AV1 S (5′ CP ORF) probe sequence without 'TT' but with the same base composition.
NG6 − TT 32mer	CGCCGCTATGCTGGCGCCTGCGCCACTACGGA	Non geminiviral oligonucleotides of 32 mer without 'TT'
dsCP	ATGTCGAAGCGACCAGCAGATATAATCATTTC TACAGCTTCGCTGGTCGTCTATATTAGTAAAG	Double stranded CP DNA probe, at 5′ terminal of CP gene
AV1S-C	TACAGCTTCGCTGGTCGTCTATATTAGTAAAG	Corresponds to complementary sequence of AV1S
Site directed mutagenesis		
C68A CP-s	GATGTTCCGCGGGAGCTGAAGGTCC	Mutation of C68 to A. The *Cfr42I* site created is underlined
C68A CP-a	GGACCTTCAGCTCCCCGCGGAACATC	
C72A CP-s	GATGTGAAGGGCCCGCTAAGGTTCAG	Mutation of C72 to A. The *ApaI* site created is underlined
C72A CP-a	CTGAACCTTAGCGGGCCCTTCACATC	
H81A CP-s	CGTTTGAGTCGCGAGCTAATATTCAG	Mutation of H81 to A. The *Bsp68I* site created is underlined
H81A CP-a	CTGAATATTAGCTCGCGACTCAAACG	
H85A CP-s	GTTTGAGTCGCGACATAATATTCAGGCTATAGG	Mutation of H85 to A. The *Bsp68I* site created is underlined
H85A CP-a	CCTATAGCCTGAATATTATGTCGCGACTCA AAC	

Restriction sites created for easy screening are underlined in the sequence and their names are given in italics.

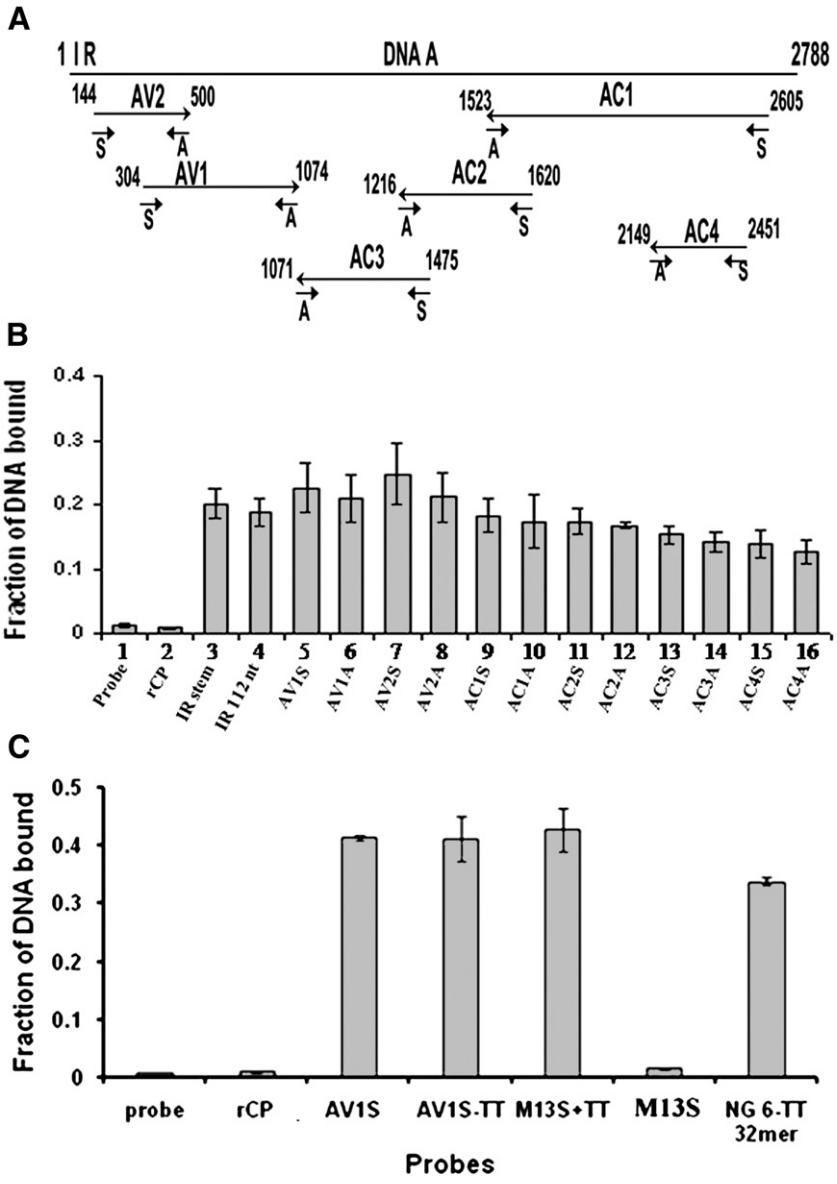

Fig. 5. (A) Schematic representation of genomic organization of DNA-A of CLCuKV-Dab. Numbers indicate the start and stop nucleotide of the open reading frame. 5′-Sense direction of the ORF and the position of the probes used are shown by long and short arrows respectively. The sense (S) and antisense (A) probes corresponding to each of the ORFs were used. (B) Binding of rCP to labeled oligonucleotides corresponding to the viral DNA sequence from different regions of the genome was analyzed by EMSA and the complex formed was quantified; the fraction of bound DNA was calculated and represented as bar diagram. Lanes 1 and 2, probe and rCP control respectively; lanes 3 to 16 represent rCP (500 ng) incubated with IRstem (2740-12), IR112nt (111–143), AV1S (304–336), AV1A (1402–1074), AV2S (144–176), AV2A (468–500), AC1S (2605–2637), AC1A (1491–1523), AC2S (1620–1652), AC2A (1184–1216), AC3S (1475–1507), AC3A (1039–1071), AC4S (2451–2483) and AC4A (2117–2149) respectively (Table 1). (C) EMSA performed with the oligonucleotides probes indicated. Lanes 1 and 2 are probe and rCP controls respectively; lanes 3–7 represent AV1S, AV1S − TT, M13S + TT, M13S and NG6 − TT 32mer respectively.

systems results in the formation of Virus-like particles (VLPs) that are purified by methods similar to that used for the purification of viruses. Such VLPs and their mutants have been used to study the assembly of viruses (Palucha et al., 2005). In the case of geminiviruses the overexpression of CP in bacterial systems has lead to misfolded insoluble protein. The CP purified under denaturing conditions and refolded is not assembly competent. The monopartite begomoviruses lack the DNA-B encoded nuclear shuttle protein (NSP), involved in the transport of viral DNA into the nucleus for replication. In these viruses, CP, which has the NLS, carries out the function of NSP and is thus involved in nuclear transport. (Hehnle et al., 2004; Kotlizky et al., 2000; Kumar et al., 2006; Kunik et al., 1998; Padidam et al., 1996). Both these functions of CP essentially involve CP–DNA interactions. Although there are a few reports on CP–DNA interactions (Hehnle et al., 2004; Kirthi and Savithri, 2003; Liu et al., 1997; Palanichelvam et al., 1998; Wege and Jeske, 1998), the kinetics of such a crucial interaction has not been investigated. In the present study, by a proper choice of pH and other parameters, the CLCuKV-Dab CP could be solubilized and purified from the soluble fraction using sucrose density gradient centrifugation (Figs. 1 and 2). However, electron microscopy of the peak fractions revealed only heterogeneous particles (data not shown) and such heterogeneous particles are not suitable for assembly studies. Attempts to obtain uniform VLPs by changing the buffer conditions and other parameters were unsuccessful. It would be interesting to examine if uniform VLPs are formed when the rCP is expressed in eukaryotic systems. However, the purified rCP that was not exposed to denaturants could be used for quantitative analysis of DNA–CP interactions.

The EMSA results clearly demonstrated that CLCuKV-Dab CP binds to AV1S ssDNA and not to M13S or dsCP probes (Fig. 3A). The CP–AV1S ssDNA probe interaction was evident from the super shift obtained upon addition of CP specific antibodies, due to the formation of CP–

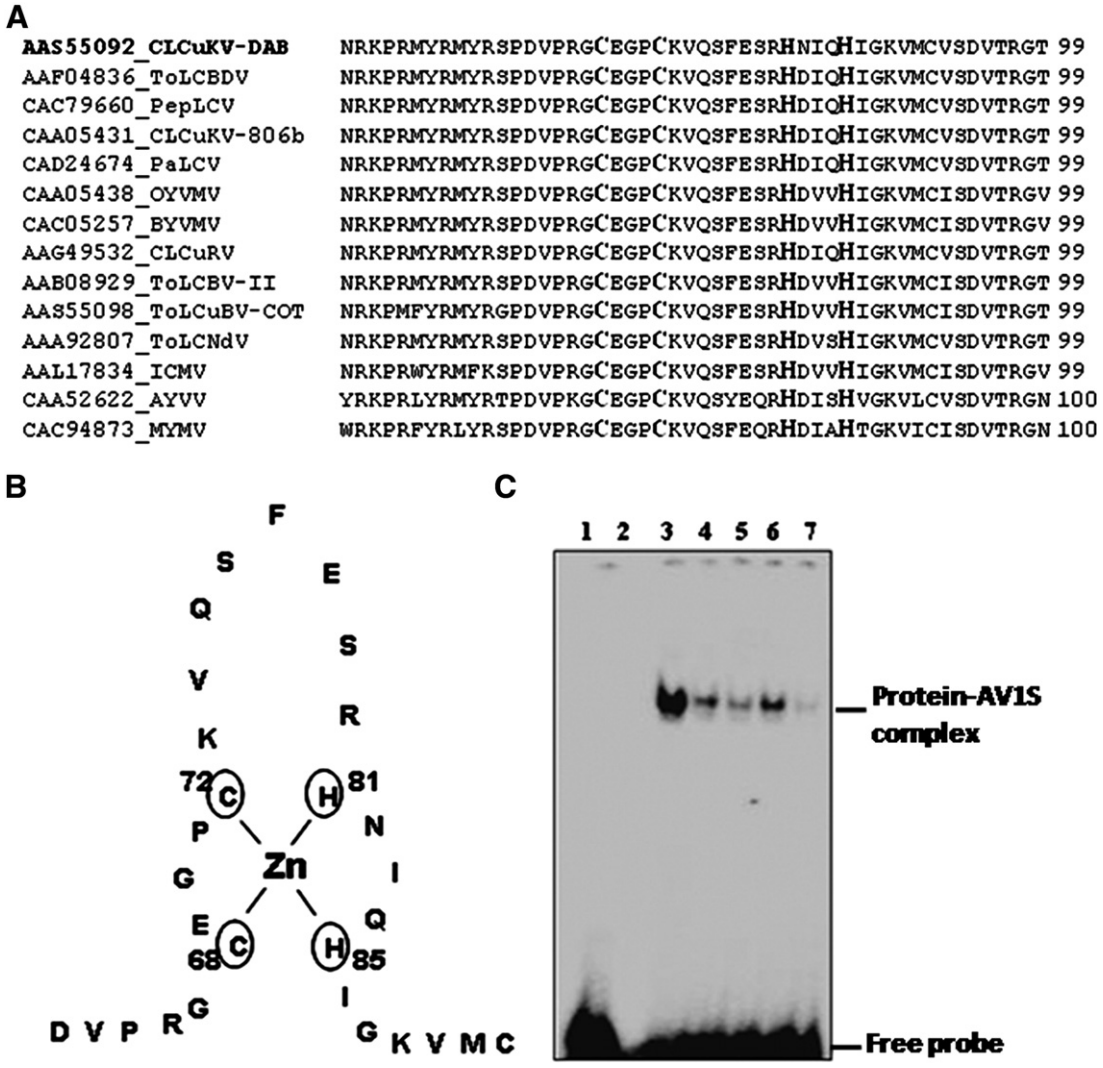

Fig. 6. Role of zinc finger motif in DNA binding. (A) Amino acid sequence alignment of conserved putative zinc finger domains of coat proteins of representative begomoviruses. Proposed residues involved in binding of zinc are shown in bold (C2H2). (B) Amino acid sequence (single letter code) in the zinc finger motif region of coat protein of CLCuKV-Dab. Conserved zinc coordinating residues are numbered to indicate their position in the full length protein. (C) PhosphorImage of the EMSA depicts the differential DNA binding properties of the zinc finger motif mutant proteins to the DNA probe. Lanes 1 and 2 are probe and rCP alone controls respectively; lanes 3–7 represent rCP–AV1S, C68A–AV1S, C72A–AV1S, H81A–AV1S and H85A–AV1S complexes respectively. The input counts (10,000 cpm) and the concentration of the protein (500 ng) used were the same in all the experiments.

DNA–antibody ternary complex (Fig. 3B) and by the competition experiments in which only the cognate cold AV1S probe and not the other non-specific probes (Fig. 3C) could chase the label. Similar studies have been carried out with refolded TYLCV CP (Palanichelvam et al., 1998). The rCP bound to AV1S probe in a concentration dependent manner (Fig. 4A). In the concentration range chosen for rCP, the binding was cooperative (Fig. 4B). Such a cooperative binding would facilitate the binding of a number of CP subunits to a single genomic ssDNA molecule, which would be essential for nuclear transport or encapsidation of the viral genome.

Although the initial EMSA results (Fig. 3) suggested that CLCuKV-Dab CP bound to AV1S and not to M13S, when DNA probes derived from various regions of the genome were tested, rCP bound to all of them (Fig. 5A). The binding was variable depending on the probe used (Fig. 5B) and the extent of binding was not correlated with the base composition of the probes or their ability to form a stem loop structure. An examination of the sequence of all the oligonucleotides used revealed that all of them had a TT in their sequence except for M13S (Table 1). In order to test if the presence of TT was essential for recognition by rCP, EMSA was performed with oligonucleotides in which TT sequence was either introduced (M13S + TT) or removed (AV1S − TT) and with a non viral oligonucleotide of same length as AV1S (NG6 − TT 32mer). The rCP could bind to all these probes except for the M13S (Fig. 5C). From the results obtained (Fig. 5), it could be concluded that the CP–DNA interaction is sequence non-specific as observed earlier (Kirthi and Savithri, 2003; Liu et al., 1997; Palanichelvam et al., 1998). The reason for the absence of binding to M13S is unclear.

The kinetics of CP–DNA interaction was examined by SPR. As evident from Figs. 7A and B, with increase in the rCP concentration, there was an increase in the response units resulting from binding of rCP to the immobilized oligonucleotide. At low concentrations of rCP (up to 15 nM) the binding and the dissociation were concentration dependent. However, at concentrations above 15 nM, there was further increase in binding which is probably due to the additional binding of rCP with lower affinity that could be removed easily during the dissociation phase. Similar observations were made even in the case of HIV-1, where the saturation of nucleocapsid protein–DNA interaction was shown to occur at 25 nM and further increase in the protein concentration resulted in additional binding of the protein to DNA with lower affinity (Fisher et al., 1998).

In the case of MSV CP, deletion of N-terminal 20 amino acids encompassing the NLS resulted in decrease in DNA binding to CP, suggesting that this region could be involved both in nuclear

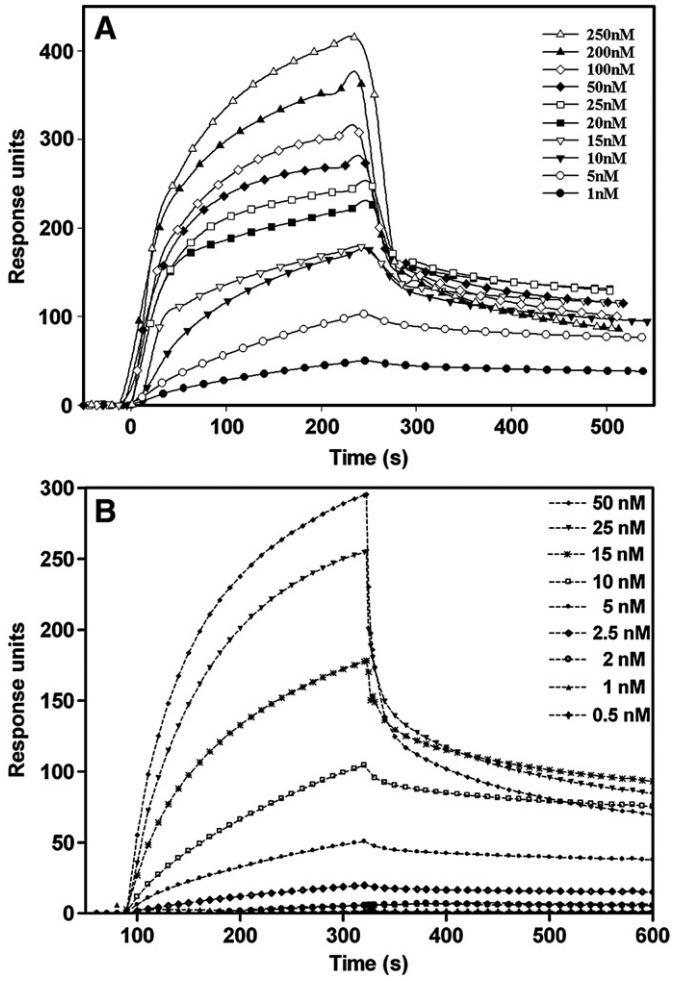

Fig. 7. SPR studies. Sensorgram showing the interaction of wild type rCP with AV1S oligonucleotide. (A) Different concentrations of rCP at 1, 5, 10, 15, 20, 25, 50, 100, 200, 250 nM and (B) at 0.5,1, 2, 2.5, 5, 10, 15, 25, 50 nM were passed over the chip containing 584 RU of immobilized biotinylated AV1S, a 32-mer ssDNA oligonucleotide. All the experiments were performed at a flow rate of 10 μl min^{-1}, allowing 240 s of association and 240 s of dissociation. *X*-axis represents the time in seconds (s) and *Y*—the response units (RU).

localization and nuclear shuttling of viral DNA (Liu et al., 1999). It is interesting to note that MSV CP lacks the zinc finger motif and hence in this case the residues at the N-terminus might mediate the CP–DNA interaction. On the other hand, in the case of ToLCBV-Ban 5 CP, it was demonstrated that the deletion of N-terminal 50 amino acid residues, including a putative α-helix and the NLS, did not affect the binding of CP to ssDNA and a conserved zinc finger motif (corresponding to residues 68–85) was responsible for CP–DNA interaction (Kirthi and Savithri, 2003). ToLCBV-Ban 5 CP and CLCuKV-Dab CP share 89.5% identity and the C2H2 motif is also conserved. The EMSA results obtained with the C68A, C72A, H81A and H85A mutants of CLCuKV-Dab CP (Fig. 6C) clearly demonstrate the significance of this motif in DNA binding. As observed earlier with ToLCBV-Ban5 CP, H85 appears to be the most important residue for CP–DNA interaction. In C2H2 type of zinc finger motif, the zinc ion is tetrahedrally coordinated by two cysteines and two histidines. Such coordination by zinc is necessary for the stability of the zinc finger and for maintaining the conformation required for DNA binding. Several studies have shown the significance of these residues in DNA binding (Cook et al., 1994; Thukral et al., 1991; Thukral et al., 1992).

In the current study, all the four zinc coordinating residues were individually mutated to alanine. Our results show that these mutations have differential effects on the DNA binding properties depending on the position of the coordinating residue (Figs. 6A and B). Mutations of the first cysteine (C68) and the final histidine (H85) of the zinc finger motif, affect the binding more drastically than the other mutations (C72A and H81A) (Fig. 8A). The 756 fold loss in k_a and the three order of magnitude decrease in affinity of H85A mutant to bind to DNA confirm that H85 is the most crucial residue (Fig. 8B). This result is consistent with earlier reports that a mutation of the final histidine in a zinc finger motif is least tolerated (Green and Sarkar, 1998; Merkle et al., 1991). The three dimensional structure of none of the monopartite begomoviruses is available except for the low resolution (16–19 Å) structure of ACMV determined by cryo electron microscopy (Bottcher et al., 2004). At this resolution, it is difficult to locate the zinc finger domain or the position of the H85.

In summary, we have used EMSA and SPR to characterize the binding of rCP to ssDNA (probes). This is the first report of kinetic analysis of the CP–DNA interaction in any geminivirus using SPR. The rCP interacts with ssDNA cooperatively in a sequence non-specific manner. Further, the rCP interacts with DNA via the zinc finger motif and mutation of the crucial H85 residue within this motif results in almost complete loss of binding to DNA. The interaction of rCP with ssDNA would be essential for the assembly of the virus and for nuclear transport.

Materials and methods

Plasmid construct

Total genomic DNA was isolated from plant leaf material infected with CLCuKV-Dab virus (Accession no: AY456683). The CP gene was amplified by PCR using the gene specific sense primer 5′CATGC-CATGGCTAGCTCGAAGCGACCAGC3′ (304) and antisense primer 5′ CGGGATCCTTACTCGAGATTTGTCACGGAATC3′ (1074). Numbers in the bracket indicate the beginning and end of the AV1 ORF respectively. The PCR (30 cycles) was performed using Deep Vent DNA polymerase with the following conditions: 94 °C for 1 min, 52 °C for 1 min and 72 °C for 45 s. The PCR product was cloned in the pRSET C vector (Invitrogen) at *NheI* and *Bam*HI sites and the clone (pRCP) was confirmed by DNA sequencing.

Generation of Zn-finger motif site directed mutants

Site-directed mutagenesis of C68, C72, H81 and H85 of the Zn-finger motif to alanine was performed by PCR based method (Weiner et al., 1994). The sense and antisense primers were designed with desired changes in the nucleotides (Table 1) and restriction sites were incorporated in the primers to enable easy screening. The mutation was confirmed by restriction analysis and by sequencing.

Expression and solubility of rCP

The recombinant clones were overexpressed in *E. coli* BL21 (DE3) pLys S (Novagen) cells. *E. coli* culture not induced with isopropyl-β-D-thiogalactoside (IPTG) and cells transformed with vector alone served as negative controls. The cells were grown at 37 °C in LB medium containing 50 μg ml^{-1} ampicillin to an optical density of 0.7 at 600 nm and induced by adding 0.5 mM IPTG for protein expression. After 3 h of induction at 30 °C, the cells were harvested and resuspended in 50 mM sodium acetate buffer (pH 5.5), with 10% glycerol and 1% Triton X-100 (Buffer A) and lysed by sonication. The debris was removed by centrifugation at 10,000 rpm for 15 min in a SS34 rotor. The pellet and the supernatant fractions were analyzed by 12% SDS-PAGE, followed by Coomassie Brilliant Blue R250 staining to determine the amount of recombinant protein in the soluble (supernatant) and insoluble (pellet) fractions. The rCP has 18 vector derived amino acids including a hexa histidine-tag at the N-terminus and two additional amino acids at the C-terminus.

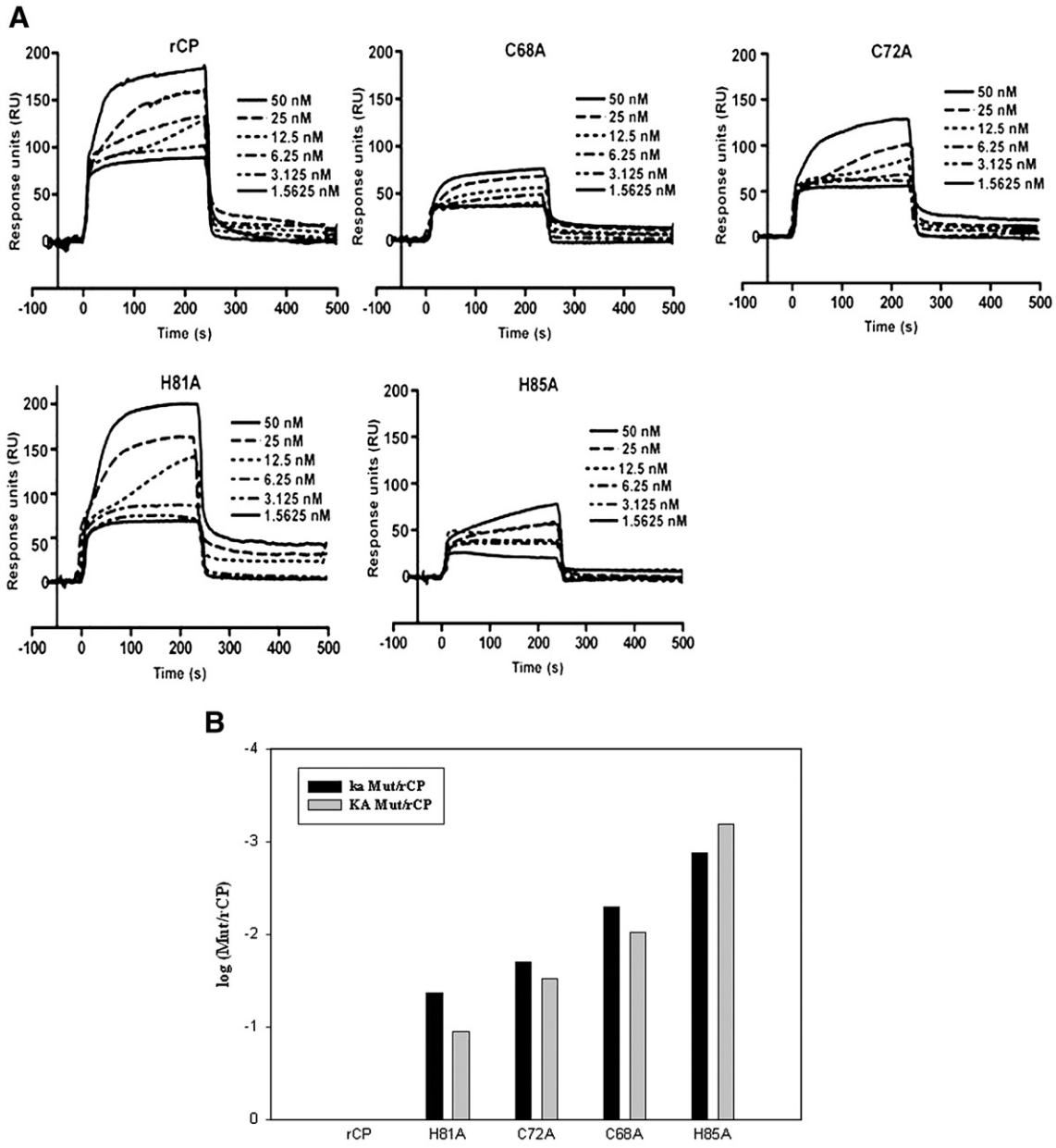

Fig. 8. SPR analysis of rCP and Zn-finger motif mutants. (A) Representative sensorgrams showing the association and dissociation profiles of rCP, C68A, C72A, H81A and H85A with AV1S. Kinetic studies were carried out with a range of protein concentrations (1.6 nM–50 nM). All the experiments were performed at a flow rate of 10 μl min^{-1}, allowing 240 s of association and 240 s of dissociation. *X*-axis represents the time in seconds (s) and *Y*–the response units (RU). (B) Graphical representation of the fold loss in association rate (k_a) and the affinity constant (K_A) for the mutants compared with rCP. The logarithm (*Y*-axis) of the fold loss in k_a and K_A are shown in black and gray bars respectively.

Protein purification

The cells from 1 l culture after induction with IPTG at 30 °C for 7–8 h were harvested by centrifugation, sonicated in buffer A and the supernatant obtained after a low speed spin was subjected to ultra-centrifugation at 140,000 *g* for 3 h using AH-629 rotor in a Sorvall Pro80 ultracentrifuge. The pellet was resuspended in a minimal volume of buffer A and layered onto preformed 10–40% sucrose density gradient prepared in 50 mM sodium acetate buffer (pH 5.5). Fractions (1.5 ml), were collected from the bottom of the tube after

Table 2
Kinetic parameters for the interaction of AV1S DNA with wild type rCP and its zinc finger motif mutants

Protein	k_a (M^{-1} s^{-1})	K_a rCP/Mut	k_d (s^{-1})	K_A (M^{-1})	K_A rCP/Mut	K_D (M)
rCP	$1.3 \pm 0.18 \times 10^{6}$	1	$4.9 \pm 1.23 \times 10^{-3}$	$2.6 \pm 0.29 \times 10^{8}$	1	$3.8 \pm 0.43 \times 10^{-9}$
H81A	$5.4 \pm 0.59 \times 10^{4}$	23	$1.9 \pm 0.24 \times 10^{-3}$	$2.8 \pm 0.01 \times 10^{7}$	9	$3.5 \pm 0.56 \times 10^{-8}$
C72A	$2.5 \pm 0.39 \times 10^{4}$	50	$3.1 \pm 0.14 \times 10^{-3}$	$8.1 \pm 1.68 \times 10^{6}$	33	$1.2 \pm 0.26 \times 10^{-7}$
C68A	$6.4 \pm 0.46 \times 10^{3}$	197	$2.5 \pm 0.23 \times 10^{-3}$	$2.6 \pm 0.05 \times 10^{6}$	104	$3.9 \pm 0.10 \times 10^{-7}$
H85A	$1.7 \pm 0.75 \times 10^{3}$	756	$1.0 \pm 0.01 \times 10^{-2}$	$1.7 \pm 0.49 \times 10^{5}$	1561	$5.9 \pm 2.16 \times 10^{-6}$

Data obtained from three independent experiments.

centrifugation at 140,000 *g* for 3 h at 4 °C. The fractions were analyzed by recording absorbance at 280 nm and by SDS-PAGE. The peak fractions (10–14) were pooled, and centrifuged at 140,000 *g* for 3 h. The pellet was resuspended in a minimal volume of 50 mM sodium acetate buffer (pH 5.5). The purity of the sample was checked by SDS-PAGE followed by staining with Coomassie Brilliant Blue (CBB R250) (Merck). The same protocol was followed for the purification of all the CP zinc finger motif mutants.

Western blot analysis

To identify the expressed and purified rCP, Western blot analysis was performed using ICMV polyclonal antibodies as the primary antibody (Kirthi and Savithri, 2003). rCP had the expected molecular mass 32 kDa and reacted well with ICMV polyclonal antibodies.

EMSA

All the oligonucleotides used in the EMSA and the competitor oligonucleotides were purchased from Sigma Chemical Co. (Table 1). ^{32}P labeled probes were prepared by 5′ end labeling of the oligonucleotides using [γ-^{32}P] ATP (BRIT) and T4 polynucleotide kinase (MBI fermentas) (Sambrook, J, Fritsch E F and Maniatis T, 1989). Unincorporated label was removed by Sephadex G-25 (Sigma) column. To generate double-stranded DNA probe, labeled sense primer was mixed with an equimolar amount of unlabeled complementary primer, denatured at 95 °C, and annealed by cooling gradually to room temperature (RT). rCP (500 ng) was incubated with 10 fmol of indicated probes (10,000 cpm) for 20 min on ice in 1× buffer B (50 mM Tris–HCl, pH 8, 100 mM NaCl, 5 mM β-mercaptoethanol, 2 mM $MgCl_2$, and 10% glycerol). DNA–protein complexes were separated from free probe by electrophoresis on 6% non-denaturing polyacrylamide gel (Native-PAGE) in 0.5× TBE buffer (45 mM Tris borate, pH 8.0, 1 mM EDTA) at 4 °C. The gels were visualized by phosphorImaging, and quantified using Imagegauge software (Fuji).

Antibody super shift experiments were performed by incubating a mixture of CP (500 ng) and ICMV polyclonal antibodies in buffer B for 10 min. on ice. This was followed by the addition of 10 fmol of probe (10,000 cpm) and further incubation of the reaction mixture on ice for 15 min. The DNA–protein complex was separated from free probe by electrophoresis as described above. For the competition assays (total volume of 20 μl), 1000 molar excess of unlabeled competitor oligonucleotide was pre-incubated in the reaction mixture prior to EMSA. In order to test the effect of protein concentration on rCP–DNA complex formation, rCP (0–500 ng), was incubated with AV1S (Table 1) oligonucleotide probe and EMSA was performed as described above. The specificity of interaction was checked by incubating various end labeled oligonucleotides (10,000 cpm) with rCP (500 ng) prior to EMSA. Similarly, rCP and the zinc finger mutant proteins (500 ng) were incubated separately with AV1S probe (10,000 cpm) and EMSA was carried out.

SPR

SPR measurements were performed according to the manufacturer's instructions in a BIAcore 2000 instrument (Pharmacia, Biosensor AB, Uppsala, Sweden) operated at 25 °C using the BIAlogue kinetics evaluation program.

AV1S oligonucleotide (Table 1) was synthesized with 5′ biotin group (MWG). Biotinylated AV1S (1.8 ng) oligonucleotide in buffer, 0.01 M HEPES, pH 7.4, 0.15 M NaCl and 0.005% surfactant P20 (running buffer) was applied to flow cells in streptavidin-derivatized sensor chips (BIAcore SA chips) at a flow rate of 2 μl min^{-1} to achieve long contact times with the surface and to control the amount of DNA bound to the surface. The sensor chips were conditioned with three consecutive 1 min injections of 100 mM NaCl (10 μl) at a flow rate of 5 μl min^{-1}, followed by extensive washing with HEPES buffer. Different concentrations of rCP (0.5–250 nM) were passed over the immobilized AV1S oligonucleotide at a flow rate of 10 μl min^{-1} and the interaction was monitored by allowing 240 s of association, followed by 240 s of dissociation. Finally the bound proteins (if any) were removed by washing with 0.01–0.1% SDS and the chip was regenerated. For each binding curve, the specific response of the AV1S surface towards rCP was obtained by subtracting the response units obtained with buffer control. For kinetic studies, SPR was performed with a range of rCP and mutant rCP concentrations (1.6–50 nM) at a flow rate of 10 μl min^{-1} in running buffer. The sensorgrams were obtained and the binding constants were derived using BIAevalution 3.1 software assuming 1:1 Langmuir binding model with mass transport. The model was chosen based on the reduced χ^2 values and the randomness of the residuals. A mass transport parameter was considered to improve the curve fitting. As a negative control, immunodepleted rCP was used. To remove rCP by immunodepletion, ICMV polyclonal antibodies (6 μg/ml) were added and incubated for 18 h at 4 °C followed by the addition of 90 μl/ml protein A-agarose and incubation for another 4 h at 4 °C. The rCP–antibody–protein A-agarose complex was pelleted by centrifugation at 10,000 rpm for 10 min, and the remaining supernatant was used for the study.

Acknowledgments

We thank Ms. Srilatha, Mr. Krishna and Mr. Saradhi Pardha for their technical assistance, Mr. Madhu N and Mr. Bandaru Murthy for their valuable discussions on BIAcore experiments. We thank Prof. V. Muniyappa for the kind gift of ICMV antibodies and Prof. Narayana Rishi for supplying CLCuKV-Dab infected leaves. We thank the Department of Biotechnology, New Delhi, India for financial support. Poornima Priyadarshini C.G thanks Council of Scientific and Industrial Research, New Delhi, India for the senior research fellowship.

Appendix A. Supplementary data

Supplementary data associated with this article can be found, in the online version, at doi:10.1016/j.virol.2009.01.016.

References

Azzam, O., Frazer, J., de la Rosa, D., Beaver, J.S., Ahlquist, P., Maxwell, D.P., 1994. Whitefly transmission and efficient ssDNA accumulation of bean golden mosaic geminivirus require functional coat protein. Virology 204 (1), 289–296.

Bisaro, D.M., 2006. Silencing suppression by geminivirus proteins. Virology 344 (1), 158–168.

Bondeson, K., Frostell-Karlsson, A., Fagerstam, L., Magnusson, G., 1993. Lactose repressor-operator DNA interactions: kinetic analysis by a surface plasmon resonance biosensor. Anal. Biochem. 214 (1), 245–251.

Bottcher, B., Unseld, S., Ceulemans, H., Russell, R.B., Jeske, H., 2004. Geminate structures of African cassava mosaic virus. J. Virol. 78 (13), 6758–6765.

Briddon, R., 2003. Cotton leaf curl disease, a multicomponent begomovirus complex. Mol. Plant Pathol. 4 (6), 427–434.

Briddon, R.W., Bull, S.E., Amin, I., Idris, A.M., Mansoor, S., Bedford, I.D., Dhawan, P., Rishi, N., Siwatch, S.S., Abdel-Salam, A.M., Brown, J.K., Zafar, Y., Markham, P.G., 2003. Diversity of DNA beta, a satellite molecule associated with some monopartite begomoviruses. Virology 312 (1), 106–121.

Briddon, R.W., Bull, S.E., Amin, I., Mansoor, S., Bedford, I.D., Rishi, N., Siwatch, S.S., Zafar, Y., Abdel-Salam, A.M., Markham, P.G., 2004. Diversity of DNA 1: a satellite-like molecule associated with monopartite begomovirus-DNA beta complexes. Virology 324 (2), 462–474.

Cook, W.J., Mosley, S.P., Audino, D.C., Mullaney, D.L., Rovelli, A., Stewart, G., Denis, C.L., 1994. Mutations in the zinc-finger region of the yeast regulatory protein ADR1 affect both DNA binding and transcriptional activation. J. Biol. Chem. 269 (12), 9374–9379.

Fisher, R.J., Rein, A., Fivash, M., Urbaneja, M.A., Casas-Finet, J.R., Medaglia, M., Henderson, L.E., 1998. Sequence-specific binding of human immunodeficiency virus type 1 nucleocapsid protein to short oligonucleotides. J. Virol. 72 (3), 1902–1909.

Fisher, R.J., Fivash, M.J., Stephen, A.G., Hagan, N.A., Shenoy, S.R., Medaglia, M.V., Smith, L.R., Worthy, K.M., Simpson, J.T., Shoemaker, R., McNitt, K.L., Johnson, D.G., Hixson,

C.V., Gorelick, R.J., Fabris, D., Henderson, L.E., Rein, A., 2006. Complex interactions of HIV-1 nucleocapsid protein with oligonucleotides. Nucleic Acids Res. 34 (2), 472–484.
Garland, P.B., 1996. Optical evanescent wave methods for the study of biomolecular interactions. Q. Rev. Biophys. 29 (1), 91–117.
Gopal, P., Pravin Kumar, P., Sinilal, B., Jose, J., Kasin Yadunandam, A., Usha, R., 2007. Differential roles of C4 and betaC1 in mediating suppression of post-transcriptional gene silencing: evidence for transactivation by the C2 of Bhendi yellow vein mosaic virus, a monopartite begomovirus. Virus Res. 123 (1), 9–18.
Green, A., Sarkar, B., 1998. Alteration of zif268 zinc-finger motifs gives rise to non-native zinc-co-ordination sites but preserves wild-type DNA recognition. Biochem. J. 333 (Pt 1), 85–90.
Hallan, V., Gafni, Y., 2001. Tomato yellow leaf curl virus (TYLCV) capsid protein (CP) subunit interactions: implications for viral assembly. Arch. Virol. 146 (9), 1765–1773.
Hatta, T., Francki, R.I., 1979. The fine structure of chloris striate mosaic virus. Virology 92 (2), 428–435.
Hehnle, S., Wege, C., Jeske, H., 2004. Interaction of DNA with the movement proteins of geminiviruses revisited. J. Virol. 78 (14), 7698–7706.
Hensley, P., Doyle, M.L., Myszka, D.G., Woody, R.W., Brigham-Burke, M.R., Erickson-Miller, C.L., Griffin, C.A., Jones, C.S., McNulty, D.E., O'Brien, S.P., Amegadzie, B.Y., MacKenzie, L., Ryan, M.D., Young, P.R., 2000. Evaluating energetics of erythropoietin ligand binding to homodimerized receptor extracellular domains. Methods Enzymol. 323, 177–207.
Hofer, P., Bedford, I.D., Markham, P.G., Jeske, H., Frischmuth, T., 1997. Coat protein gene replacement results in whitefly transmission of an insect nontransmissible geminivirus isolate. Virology 236 (2), 288–295.
Hohnle, M., Hofer, P., Bedford, I.D., Briddon, R.W., Markham, P.G., Frischmuth, T., 2001. Exchange of three amino acids in the coat protein results in efficient whitefly transmission of a nontransmissible Abutilon mosaic virus isolate. Virology 290 (1), 164–171.
Kirthi, N., Maiya, S.P., Murthy, M.R., Savithri, H.S., 2002. Evidence for recombination among the tomato leaf curl virus strains/species from Bangalore, India. Arch. Virol. 147 (2), 255–272.
Kirthi, N., Priyadarshini, C.G., Sharma, P., Maiya, S.P., Hemalatha, V., Sivaraman, P., Dhawan, P., Rishi, N., Savithri, H.S., 2004. Genetic variability of begomoviruses associated with cotton leaf curl disease originating from India. Arch. Virol. 149 (10), 2047–2057.
Kirthi, N., Savithri, H.S., 2003. A conserved zinc finger motif in the coat protein of Tomato leaf curl Bangalore virus is responsible for binding to ssDNA. Arch. Virol. 148 (12), 2369–2380.
Klug, A., Schwabe, J.W., 1995. Protein motifs 5. Zinc fingers. FASEB J. 9 (8), 597–604.
Kotlizky, G., Boulton, M.I., Pitaksutheepong, C., Davies, J.W., Epel, B.L., 2000. Intracellular and intercellular movement of maize streak geminivirus V1 and V2 proteins transiently expressed as green fluorescent protein fusions. Virology 274 (1), 32–38.
Kumar, P.P., Usha, R., Zrachya, A., Levy, Y., Spanov, H., Gafni, Y., 2006. Protein–protein interactions and nuclear trafficking of coat protein and betaC1 protein associated with Bhendi yellow vein mosaic disease. Virus Res. 122 (1–2), 127–136.
Kunik, T., Palanichelvam, K., Czosnek, H., Citovsky, V., Gafni, Y., 1998. Nuclear import of the capsid protein of tomato yellow leaf curl virus (TYLCV) in plant and insect cells. Plant J. 13 (3), 393–399.
Lazarowitz, S.G., 1992. Geminivirus: genome structure and gene function. Crit. Rev. Plant Sci. 11, 327–349.
Liu, H., Boulton, M.I., Davies, J.W., 1997. Maize streak virus coat protein binds single- and double-stranded DNA in vitro. J. Gen. Virol. 78 (Pt 6), 1265–1270.
Liu, H., Boulton, M.I., Thomas, C.L., Prior, D.A., Oparka, K.J., Davies, J.W., 1999. Maize streak virus coat protein is karyophyllic and facilitates nuclear transport of viral DNA. Mol. Plant-Microb. Interact. 12 (10), 894–900.
Mackay, J.P., Crossley, M., 1998. Zinc fingers are sticking together. Trends Biochem. Sci. 23 (1), 1–4.
Merkle, D.L., Schmidt, M.H., JM, B., 1991. Design and chacterization of a ligand-binding metellopeptide. J. Am. Chem. Soc. 113, 5450–5451.
Myszka, D.G., 2000. Kinetic, equilibrium, and thermodynamic analysis of macromolecular interactions with BIACORE. Methods Enzymol. 323, 325–340.
Nice, E.C., Catimel, B., 1999. Instrumental biosensors: new perspectives for the analysis of biomolecular interactions. BioEssays 21 (4), 339–352.
Noris, E., Vaira, A.M., Caciagli, P., Masenga, V., Gronenborn, B., Accotto, G.P., 1998. Amino acids in the capsid protein of tomato yellow leaf curl virus that are crucial for systemic infection, particle formation, and insect transmission. J. Virol. 72 (12), 10050–10057.
O'Shannessy, D.J., 1994. Determination of kinetic rate and equilibrium binding constants for macromolecular interactions: a critique of the surface plasmon resonance literature. Curr. Opin. Biotechnol. 5 (1), 65–71.
Oda, M., Furukawa, K., Sarai, A., Nakamura, H., 1999. Kinetic analysis of DNA binding by the c-Myb DNA-binding domain using surface plasmon resonance. FEBS Lett. 454 (3), 288–292.
Padidam, M., Beachy, R.N., Fauquet, C.M., 1996. The role of AV2 ("precoat") and coat protein in viral replication and movement in tomato leaf curl geminivirus. Virology 224 (2), 390–404.
Palanichelvam, K., Kunik, T., Citovsky, V., Gafni, Y., 1998. The capsid protein of tomato yellow leaf curl virus binds cooperatively to single-stranded DNA. J. Gen. Virol. 79 (Pt 11), 2829–2833.
Palucha, A., Loniewska, A., Satheshkumar, S., Boguszewska-Chachulska, A.M., Umashankar, M., Milner, M., Haenni, A.L., Savithri, H.S., 2005. Virus-like particles: models for assembly studies and foreign epitope carriers. Prog. Nucleic Acid Res. Mol. Biol. 80, 135–136.
Rojas, M.R., Jiang, H., Salati, R., Xoconostle-Cazares, B., Sudarshana, M.R., Lucas, W.J., Gilbertson, R.L., 2001. Functional analysis of proteins involved in movement of the monopartite begomovirus, tomato yellow leaf curl virus. Virology 291 (1), 110–125.
Shastry, B.S., 1996. Transcription factor IIIA (TFIIIA) in the second decade. J. Cell. Sci. 109 (Pt 3), 535–539.
Silin, Plant, 1997. Biotechnological applications of surface plasmon resonance. Trends Biotechnol. 15, 353–359.
Stanley, J., Townsend, R., 1985. Characterisation of DNA forms associated with cassava latent virus infection. Nucleic Acids Res. 13 (7), 2189–2206.
Stanley, J., Bisaro, D.M., Briddon, R.W., Brown, J.K., Fauquet, C.M., Harrison, B.D., Rybicki, E.P., Stenger, D.C., 2005. Geminiviridae. In: Fauquet, C.M., Mayo, M.A., Maniloff, J., Desselberger, U., Ball, L.A. (Eds.), Virus Taxonomy. VIIIth Report of the International Committee on Taxonomy of Viruses. Elsevier/Academic Press, London.
Thukral, S.K., Morrison, M.L., Young, E.T., 1991. Alanine scanning site-directed mutagenesis of the zinc fingers of transcription factor ADR1: residues that contact DNA and that transactivate. Proc. Natl. Acad. Sci. U.S.A. 88 (20), 9188–9192.
Thukral, S.K., Morrison, M.L., Young, E.T., 1992. Mutations in the zinc fingers of ADR1 that change the specificity of DNA binding and transactivation. Mol. Cell. Biol. 12 (6), 2784–2792.
Tsoi, P.Y., Yang, M., 2002. Kinetic study of various binding modes between human DNA polymerase beta and different DNA substrates by surface-plasmon-resonance biosensor. Biochem. J. 361 (Pt 2), 317–325.
Unseld, S., Frischmuth, T., Jeske, H., 2004. Short deletions in nuclear targeting sequences of African cassava mosaic virus coat protein prevent geminivirus twinned particle formation. Virology 318 (1), 90–101.
Van Regenmortel, M.H., Mayo, M.A., Fauquet, C.M., Maniloff, J., 2000. Virus nomenclature: consensus versus chaos. Arch. Virol. 145 (10), 2227–2232.
Wartig, L., Kheyr-Pour, A., Noris, E., De Kouchkovsky, F., Jouanneau, F., Gronenborn, B., Jupin, I., 1997. Genetic analysis of the monopartite tomato yellow leaf curl geminivirus: roles of V1, V2, and C2 ORFs in viral pathogenesis. Virology 228 (2), 132–140.
Wege, C., Jeske, H., 1998. Abutilon mosaic geminivirus proteins expressed and phosphorylated in *Escherichia coli*. J. Phytopathol. 146, 613–621.
Weiner, M.P., Costa, G.L., Schoettlin, W., Cline, J., Mathur, E., Bauer, J.C., 1994. Site-directed mutagenesis of double-stranded DNA by the polymerase chain reaction. Gene 151 (1–2), 119–123.
Yamamoto, A., Ando, Y., Yoshioka, K., Saito, K., Tanabe, T., Shirakawa, H., Yoshida, M., 1997. Difference in affinity for DNA between HMG proteins 1 and 2 determined by surface plasmon resonance measurements. J. Biochem. (Tokyo) 122 (3), 586–594.
Yoshioka, K., Saito, K., Tanabe, T., Yamamoto, A., Ando, Y., Nakamura, Y., Shirakawa, H., Yoshida, M., 1999. Differences in DNA recognition and conformational change activity between boxes A and B in HMG2 protein. Biochemistry 38 (2), 589–595.
Zhang, W., Olson, N.H., Baker, T.S., Faulkner, L., Agbandje-McKenna, M., Boulton, M.I., Davies, J.W., McKenna, R., 2001. Structure of the Maize streak virus geminate particle. Virology 279 (2), 471–477.